Letter

Small-Signal Modeling of Three-Phase Synchronous Reference Frame Phase-Locked Loops

Florian Hans, Walter Schumacher, and Lennart Harnefors, *Fellow, IEEE*

***Abstract*—Synchronous reference frame (SRF) phase-locked loops (PLLs) represent a commonly used technique for grid synchronization in distributed generation (DG) systems. Since PLLs affect transient dynamics, they are a crucial component for stability studies. In this letter, it is shown that a commonly used small-signal SRF-PLL model can be used for stability analysis in some preconditioned scenarios with a single grid-connected DG unit, but does necessarily require perturbation quantities that are offset free. Otherwise, an incorrect usage may result in unacceptable errors. To overcome this restriction, an improved small-signal PLL model is proposed, which enables to analyze the effects of grid frequency and phase angle changes as well as variations of the input voltage magnitude. Finally, the model accuracy is validated by means of computer simulations.**

***Index Terms*—Distributed generation (DG), phase-locked loop (PLL), small-signal modeling, synchronization, voltage source converter (VSC).**

I. Introduction

In RECENT years, renewable energy sources have become important in many countries enabling a growing sustainable energy production. Many distributed generation (DG) units use voltage source converters (VSCs) as a grid-connecting interface [1]. While present VSCs that operate as current sources typically apply phase-locked loop (PLL) techniques for grid synchronization [1], [2], PLLs can also be implemented by any other DG unit to offer ancillary services like the provision of frequency response [3].

Since PLLs represent a key component in many DG systems, an adequate modeling is crucial for stability analysis as well as for controller design. Even though there exist a large variety of PLL techniques (see, e.g., [2]), the basic model of a synchronous reference frame (SRF)-PLL is sufficiently accurate to represent the fundamental phase angle tracking process in many research works [3]–[10].

Manuscript received October 11, 2017; revised November 10, 2017; accepted November 30, 2017. Date of publication December 12, 2017; date of current version March 5, 2018. *(Corresponding author: Florian Hans.)*

F. Hans and W. Schumacher are with the Institute of Control Engineering, Technische Universität Braunschweig, Braunschweig 38106, Germany (e-mail: hans@ifr.ing.tu-bs.de; w.schumacher@tu-bs.de).

L. Harnefors is with the ABB Corporate Research, Västerås 72178, Sweden (e-mail: lennart.harnefors@se.abb.com).

Color versions of one or more of the figures in this letter are available online at http://ieeexplore.ieee.org.

Digital Object Identifier 10.1109/TPEL.2017.2783189

For design purposes, most authors use a linearization with instantaneous voltage phase angle as input and estimated phase angle as output [2], [5]. This phase-error model shows the dynamical behavior of a classical linear second-order system allowing a simple controller design, e.g., referring to a desired closed-loop system bandwidth or settling time. Nevertheless, since (as for the nonlinear structure) a three-phase voltage serves as PLL input, this model is not applicable in most transient studies. Thus, a simplified representation in space vector notation is preferable, especially thinking about simulation studies involving a high number of DG units.

Harnefors *et al.* [6] and Wen *et al.* [7] derive a small-signal SRF-PLL model that relates a voltage input perturbation to the phase angle error between estimated and actual phase angle. Meanwhile, this model has been acquired in many proceeding works, e.g., [8] and [9] and is applied by other authors [4], [10], showing that the model is well accepted among researchers.

However, requiring that there exists a steady-state input voltage, which is known beforehand and that the voltage perturbation is free of an offset, the applicability is restricted to some preconditioned scenarios that are not given in general. An incorrect usage as linearization around an arbitrary operating point may result in quantities that are not free of offsets and thus in unacceptable errors. Moreover, it is demonstrated that the model is suitable in analyses concerning a single grid-connected VSC, but not readily applicable in studies involving multiple DG units. Hence, in order to remove the revealed drawbacks of the modeling approach in [6] and [7], a new small-signal SRF-PLL model is proposed and validated by means of computer simulations.

II. PLL Modeling Based on Voltage Perturbation

In this section, the basic modeling idea of [6] and [7] is reviewed. For convenience, the derivation of [6] is adopted exemplary, but is slightly changed in notation to increase comprehensibility. Hereby, each three-phase quantity can equivalently be expressed as complex space vector in stationary (α, β)-coordinates, which are denoted as $\boldsymbol{v}^s = v_\alpha + jv_\beta$, or with respect to any rotating (d, q)-reference frame by $\boldsymbol{v} = e^{-j\nu}\boldsymbol{v}^s = v_d + jv_q$, where ν is the rotation angle.

Regarding the control of grid-connected VSCs, each converter implements a synchronization loop to estimate the voltage phase angle θ_i and angular frequency $\omega_i = \frac{d\theta_i}{dt}$ at the point of common coupling (PCC). To do so, the standard three-phase

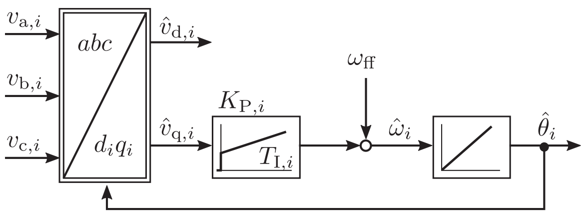

Fig. 1. Principle structure of a three-phase SRF-PLL.

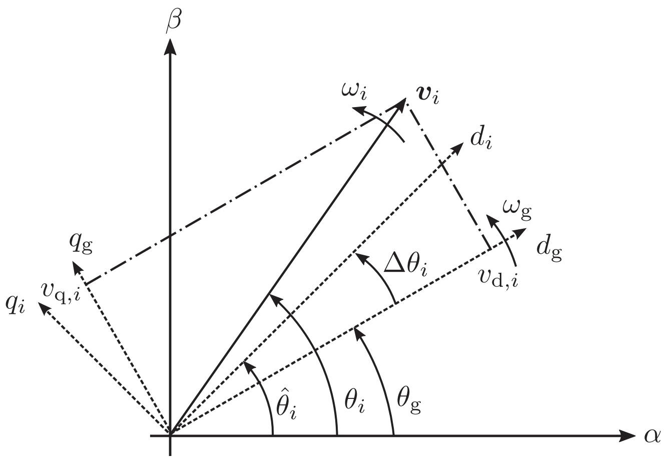

Fig. 2. Voltage space vector, converter, and grid reference frames with associated phase angles.

SRF-PLL structure shown in Fig. 1 can be used. Given a measured PCC input voltage $\boldsymbol{v}_i^s$, the control objective is to rotate a (d_i, q_i)-reference frame, such that the d_i-axis will be aligned with the voltage space vector $\boldsymbol{v}_i^s$ and the estimated phase angle $\hat{\theta}_i$ will be equal to the voltage phase angle θ_i.

For grid stability studies, it is convenient to relate all quantities to a common grid (d_g, q_g)-reference frame, which is defined by the instantaneous phase angle θ_g and a constant angular frequency $\omega_g = \frac{d}{dt}\theta_g = \text{const}$. As illustrated in Fig. 2, the PCC input voltage $\boldsymbol{v}_i^s$ can be expressed in terms of grid coordinates as $\boldsymbol{v}_i = e^{-j\theta_g}\boldsymbol{v}_i^s$. On the other hand, $\boldsymbol{v}_i^s$ can also be related to the converters (d_i, q_i)-reference frame, i.e., $\hat{\boldsymbol{v}}_i = e^{-j\hat{\theta}_i}\boldsymbol{v}_i^s$, where the ˆ-symbol denotes quantities in local converter coordinates that are associated with the estimated phase angle $\hat{\theta}_i$ provided by the ith PLL. Now, following the reasoning of [6], $\boldsymbol{v}_i^s$ can be eliminated by

$$\hat{\boldsymbol{v}}_i = e^{-j\hat{\theta}_i}\boldsymbol{v}_i^s = e^{-j\hat{\theta}_i}e^{j\theta_g}\boldsymbol{v}_i = e^{-j\Delta\theta_i}\boldsymbol{v}_i, \quad \Delta\theta_i = \hat{\theta}_i - \theta_g \tag{1}$$

where $\Delta\theta_i$ is the error angle between the ith converter and grid frame. Then, assuming only small error angles and supposing that the input voltage vector can be decomposed as $\boldsymbol{v}_i = v_{d,i}^* + \Delta\boldsymbol{v}_i$, where $v_{d,i}^*$ represents the steady-state value and $\Delta\boldsymbol{v}_i$ a small voltage perturbation, that is free of any offset, (1) can be approximated by

$$\begin{aligned}\hat{\boldsymbol{v}}_i &= e^{-j\Delta\theta_i}\boldsymbol{v}_i \approx (1 - j\Delta\theta_i)(v_{d,i}^* + \Delta\boldsymbol{v}_i)\\ &\approx v_{d,i}^* + \Delta\boldsymbol{v}_i - jv_{d,i}^*\Delta\theta_i.\end{aligned} \tag{2}$$

Reviewing the control scheme in Fig. 1, where a proportional-integral (PI) controller is used to regulate the $\hat{v}_{q,i}$-component to zero, the PLL dynamics are given by

$$\frac{d}{dt}\hat{\theta}_i = \omega_{ff} + \left(K_{P,i}\,\mathrm{Im}\{\hat{\boldsymbol{v}}_i\} + K_{I,i}\int_0^t \mathrm{Im}\{\hat{\boldsymbol{v}}_i\}\,d\tau\right) \tag{3}$$

where $K_{P,i}, K_{I,i}$ are the controller PI gain, respectively, and ω_{ff} is a constant feed-forward action, e.g., $2\pi 50\,\frac{\text{rad}}{\text{s}}$ or $2\pi 60\,\frac{\text{rad}}{\text{s}}$. Substituting (2) into (3), the dynamics of $\Delta\theta_i = \hat{\theta}_i - \theta_g$ in the Laplace domain become

$$s\Delta\theta_i(s) = G_{PI,i}(s)\left[\mathrm{Im}\{\Delta\boldsymbol{v}_i(s)\} - v_{d,i}^*\Delta\theta_i(s)\right] \tag{4}$$

where it is assumed that ω_{ff} compensates for the constant angular frequency $\frac{d}{dt}\theta_g = \omega_g$ and $G_{PI,i}(s)$ is the transfer function of the PI controller, i.e.,

$$G_{PI,i}(s) = K_{P,i} + \frac{K_{I,i}}{s} = K_{P,i}\frac{T_{I,i}s + 1}{T_{I,i}s} \tag{5}$$

with $T_{I,i} = \frac{K_{P,i}}{K_{I,i}}$ as integral time. Finally, rearranging (4) yields the existing small-signal SRF-PLL model $G_{PLL,i}(s)$ that is given by

$$\begin{aligned}\Delta\theta_i(s) &= \overbrace{\frac{G_{PI,i}(s)}{s + v_{d,i}^* G_{PI,i}(s)}}^{G_{PLL,i}(s)}\mathrm{Im}\{\Delta\boldsymbol{v}_i(s)\}\\ &= \frac{K_{P,i}s + K_{I,i}}{s^2 + v_{d,i}^* K_{P,i}\,s + v_{d,i}^* K_{I,i}}\mathrm{Im}\{\Delta\boldsymbol{v}_i(s)\}.\end{aligned} \tag{6}$$

III. Problem Statement

Reviewing the basic objective of a synchronization loop, the PLL structure forces the error between estimated phase angle $\hat{\theta}_i$ and actual angle θ_i asymptotically to zero. Since the error angle $\Delta\theta_i = \hat{\theta}_i - \theta_g$ involves the grid angle θ_g, the PLL model output $\Delta\theta_i$ will only become zero if the imaginary part of the input voltage perturbation $\mathrm{Im}\{\Delta\boldsymbol{v}_i\}$ does not contain any offset, i.e., $\lim_{t\to\infty}\boldsymbol{v}_i = v_{d,i}^*$. Hence, the applicability of the existing SRF-PLL model (6) is restricted to stability analysis, where the PCC voltage perturbation $\Delta\boldsymbol{v}_i$ serves as system input and the exact steady-state values are known beforehand.

In contrast, if the DG unit is connected to the grid over a grid impedance and outer control loops are considered, the PCC voltage cannot be used as system input, but rather as a system state, which is influenced by the injected current. Especially if the analysis involves multiple grid-connected DG units, an exact analytical calculation of the steady-state values is often impossible due to implicit nonlinear equations and a numerical approximation has to be considered, probably violating $\lim_{t\to\infty}\boldsymbol{v}_i = v_{d,i}^*$. Then, the existing PLL model can formally not be used for stability analysis.

This is due to the fact that (6) represents a linearization that depends on the chosen grid reference frame. If the grid (d_g, q_g)-reference frame is not aligned with the PCC voltage in the steady state, the tracking error $\hat{\theta}_i - \theta_i$ of the small-signal model does not vanish and (6) is not a valid PLL model. It is to be emphasized that the usage of (6) as a linearized PLL model may lead to unreasonable results for any operating point $v_{d,i,0}$, which does not represent the steady-state PCC voltage $v_{d,i}^*$. Particularly, this

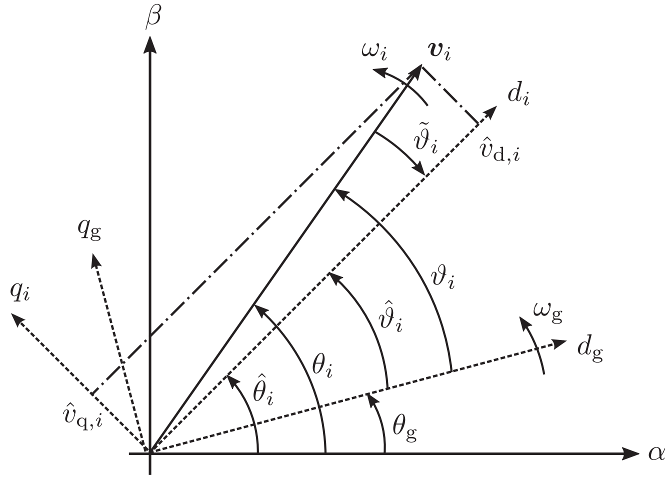

Fig. 3. Definition of absolute and relative phase angles.

might be the case in (simulative) transient studies, where a stiff grid is considered as a reference.

Therefore, a generally valid linearization of the nonlinear SRF-PLL structure in Fig. 1 is motivated, that does not impose a restriction on the chosen grid reference frame. In fact, the discussed difficulties can be overcome by the definition of a different error angle utilizing relative phase angles that are related to any common rotating grid (d_g, q_g)-reference frame instead of the stationary (α, β)-frame.

IV. Proposed Small-Signal PLL Model

In order to define a new error angle, absolute and relative phase angles are introduced first. As shown in Fig. 3, the definitions of θ_i and $\hat{\theta}_i$ remain the same as for the existing PLL model (6). In addition, the relative phase angles $\vartheta_i = \theta_i - \theta_g$ and $\hat{\vartheta}_i = \hat{\theta}_i - \theta_g$ (which is equal to $\Delta\theta_i$) are considered to describe the rotation of the voltage space vector $\boldsymbol{v}_i$ and the converter (d_i, q_i)-frame to the grid (d_g, q_g)-reference frame, respectively. Hence, each voltage space vector $\boldsymbol{v}_i$ can be expressed in converter coordinates as

$$\hat{\boldsymbol{v}}_i = e^{-j\hat{\vartheta}_i}\boldsymbol{v}_i = e^{-j\hat{\vartheta}_i}e^{j\vartheta_i}\,|\boldsymbol{v}_i| = e^{-j\tilde{\vartheta}_i}\,|\boldsymbol{v}_i|\,, \quad \tilde{\vartheta}_i = \hat{\vartheta}_i - \vartheta_i \tag{7}$$

where $\tilde{\vartheta}_i$ defines the new error angle between the estimated and actual relative phase angle and $|\boldsymbol{v}_i|$ is the (measured) magnitude of the voltage vector $\boldsymbol{v}_i$. At this point, it should be noted that $\tilde{\vartheta}_i = \hat{\vartheta}_i - \vartheta_i = \hat{\theta}_i - \theta_i$ will become zero in the steady state, and thus, $\hat{v}_{d,i}$ seen by the converter will be equal to the voltage magnitude $|\boldsymbol{v}_i|$. Using the PLL dynamics (3), which can be decomposed as

$$\frac{d}{dt}\hat{\theta}_i = \frac{d}{dt}\hat{\vartheta}_i + \omega_g = \omega_{\mathrm{ff}} + \left(K_{P,i}\,\mathrm{Im}\left\{\hat{\boldsymbol{v}}_i\right\} + K_{I,i}\int_0^t \mathrm{Im}\left\{\hat{\boldsymbol{v}}_i\right\}d\tau\right) \tag{8}$$

and substituting (7) into (8), after rearranging, the dynamics of the estimated relative phase angle $\hat{\vartheta}_i$ are determined by

$$\frac{d}{dt}\hat{\vartheta}_i = \omega_{\mathrm{ff}} - \omega_g - \left(K_{P,i}\,|\boldsymbol{v}_i|\sin(\tilde{\vartheta}_i) + K_{I,i}\int_0^t |\boldsymbol{v}_i|\sin(\tilde{\vartheta}_i)d\tau\right). \tag{9}$$

Then, observing that $\vartheta_i = \arctan\left(\frac{v_{q,i}}{v_{d,i}}\right)$ with time derivative

$$\frac{d}{dt}\vartheta_i = -\frac{v_{q,i}}{|\boldsymbol{v}_i|^2}\frac{d}{dt}v_{d,i} + \frac{v_{d,i}}{|\boldsymbol{v}_i|^2}\frac{d}{dt}v_{q,i} \tag{10}$$

the nonlinear residual dynamics of the error angle $\tilde{\vartheta}_i$, i.e., $\frac{d}{dt}\tilde{\vartheta}_i = f_i(\tilde{\vartheta}_i, \omega_g, \boldsymbol{v}_i, \dot{\boldsymbol{v}}_i) = \frac{d}{dt}\hat{\vartheta}_i - \frac{d}{dt}\vartheta_i$, are specified by (9) and (10). Hereby, $\tilde{\vartheta}_i$ represents the state variable and ω_g, $\boldsymbol{v}_i$, and $\dot{\boldsymbol{v}}_i = \frac{d}{dt}\boldsymbol{v}_i$ are the system's inputs.

Now, considering small changes of the state variable $\tilde{\vartheta}_i$ and the input $\boldsymbol{u}_i = [\omega_g, \boldsymbol{v}_i, \dot{\boldsymbol{v}}_i]^T$ around an operating point $\tilde{\vartheta}_{i,0}, \boldsymbol{u}_{i,0}$, a small-signal linearization of the form

$$\Delta\dot{\tilde{\vartheta}}_i = \left.\frac{\partial f_i}{\partial\tilde{\vartheta}_i}\right|_{\tilde{\vartheta}_{i,0},\boldsymbol{u}_{i,0}}\Delta\tilde{\vartheta}_i + \left.\frac{\partial f_i}{\partial\boldsymbol{u}_i}\right|_{\tilde{\vartheta}_{i,0},\boldsymbol{u}_{i,0}}\Delta\boldsymbol{u}_i \tag{11}$$

where $\Delta\tilde{\vartheta}_i = \tilde{\vartheta}_i - \tilde{\vartheta}_{i,0}$ and $\Delta\boldsymbol{u}_i = \boldsymbol{u}_i - \boldsymbol{u}_{i,0}$ can be developed. Given (9), (10) and taking $\tilde{\vartheta}_{i,0} = 0$, $\boldsymbol{u}_{i,0} = [\omega_{g,0}, \boldsymbol{v}_{i,0}, \boldsymbol{0}]^T$ as operating point, and $\omega_{\mathrm{ff}} = \omega_{g,0}$, the linearized PLL dynamics in the Laplace domain are given by

$$\begin{aligned} s\Delta\tilde{\vartheta}_i(s) = &-\Delta\omega_g(s) - |\boldsymbol{v}_{i,0}|\,G_{\mathrm{PI},i}(s)\Delta\tilde{\vartheta}_i(s) \\ &+ k_{q,i}\,s\,\Delta v_{d,i}(s) - k_{d,i}\,s\,\Delta v_{q,i}(s) \end{aligned} \tag{12}$$

where

$$k_{q,i} = \frac{v_{q,i,0}}{|\boldsymbol{v}_{i,0}|^2}, \qquad k_{d,i} = \frac{v_{d,i,0}}{|\boldsymbol{v}_{i,0}|^2}. \tag{13}$$

Finally, rearranging (12), the resulting small-signal SRF-PLL dynamics are given by

$$\begin{aligned} \Delta\tilde{\vartheta}_i(s) = &-\frac{1}{s + |\boldsymbol{v}_{i,0}|\,G_{\mathrm{PI},i}(s)}\Delta\omega_g(s) \\ &+ \frac{k_{q,i}s}{s + |\boldsymbol{v}_{i,0}|\,G_{\mathrm{PI},i}(s)}\mathrm{Re}\left\{\Delta\boldsymbol{v}_i(s)\right\} \\ &- \frac{k_{d,i}s}{s + |\boldsymbol{v}_{i,0}|\,G_{\mathrm{PI},i}(s)}\mathrm{Im}\left\{\Delta\boldsymbol{v}_i(s)\right\}. \end{aligned} \tag{14}$$

Here, $|\boldsymbol{v}_{i,0}|$ may be the steady-state value $v^*_{d,i}$, but also any other operating point. Comparing the existing PLL model (6) with (14), it can be observed that $G_{\mathrm{PI},i}(s)$ in the numerator of $G_{\mathrm{PLL},i}(s)$ introduces a proportional-derivative action that is not present in (14), where $G_{\mathrm{PI},i}(s)$ does only appear in the denominator. Given the slightly different model (14), $\Delta\tilde{\vartheta}_i$ will become zero and the PLL will track the phase angle θ_i in the steady-state for any step change of the grid frequency $\Delta\omega_g$ due to the integral part of the PI controller and ramp changes of $\Delta v_{d,i}, \Delta v_{q,i}$. Hence, (14) represents an extension of (6), where grid frequency and phase angle changes as well as variations of the PCC voltage magnitude can be analyzed.

Moreover, since the relative phase angle $\Delta\tilde{\vartheta}_i$ is independent of the grid (d_g, q_g)-reference frame, i.e., θ_g, the proposed model does not impose any restriction on the chosen grid reference. The reference frame does no longer have to be close to the PCC voltage vector, and thus, (14) can readily be used in studies

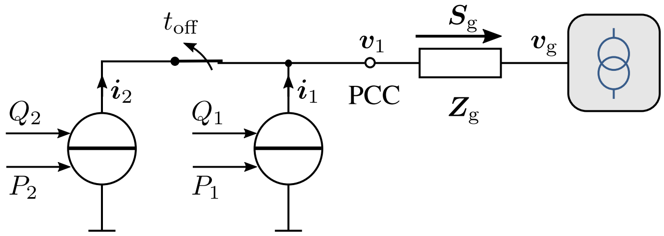

Fig. 4. Exemplary system of two grid-connected DG units.

concerning multiple DG units without defining an associated steady-state grid reference frame at each PCC.

V. Simulation Results

To demonstrate the discussed problems that are related to the existing PLL model of Section II and to validate the proposed model, the phase tracking process has been tested by means of computer simulations. Therefore, an exemplary system consisting of two DG units that are modeled as ideal current sources, which are connected to the power grid over a common grid impedance at the same PCC, as depicted in Fig. 4, is considered. Supposing that both units are initially connected to the grid injecting a constant current, the disconnection of the second unit (e.g., due to a line fault or an emergency shutdown) will result in a sudden phase change as well as in a decrease of the PCC voltage magnitude.

In the tested scenarios, both DG units are equipped with the same standard three-phase PLL in Fig. 1, where the PI controller design has been adopted from [5], i.e., $K_{P,1} = \frac{2\zeta_{\text{cl}}\omega_{\text{cl}}}{|\boldsymbol{v}_{1,0}|}$, $K_{I,1} = \frac{\omega_{\text{cl}}^2}{|\boldsymbol{v}_{1,0}|}$, with $\zeta_{\text{cl}}, \omega_{\text{cl}}$ as damping ratio and closed-loop PLL bandwidth, respectively. The PCC voltage magnitude before the fault is $|\boldsymbol{v}_{1,0}| = 311\,\text{V}$, while the grid frequency is assumed to be constant at $\omega_g = \omega_{\text{ff}} = 2\pi 50\,\frac{\text{rad}}{\text{s}}$.

If the (d_g, q_g)-reference frame is defined to be aligned with the PCC voltage vector in the steady-state, i.e., $v_{d,1}^* \hat{=} v_{d,1,0}$, $v_{q,1,0} = 0$, the existing as well as the proposed model track the fault equally accurately and match with the nonlinear system, but is not shown here due to space limitations. However, if the gird (d_g, q_g)-reference frame is initially aligned with $\boldsymbol{v}_1$, a fault will result in a voltage perturbation showing an offset of the form $\Delta\boldsymbol{v}_1 = e^{j\delta}\,|\boldsymbol{v}_1| - v_{d,1,0}$, where δ in rad is the amount of the phase change. Defining $v_{d,1}^* \hat{=} |\boldsymbol{v}_{1,0}| = v_{d,1,0} = 311\,\text{V}, v_{q,1,0} = 0\,\text{V}$ as operating point and supposing that the disconnection of the second DG unit at $t_{\text{off}} = 3\,\text{ms}$ yields a sudden phase change of $\delta = -10^\circ$ with a 2% decrease of the PCC voltage magnitude to $|\boldsymbol{v}_1| = 305\,\text{V}$, Fig. 5 shows a detailed section of the resulting phase angle difference $\hat{\theta}_1 - \theta_g$ for two different PLL parameter settings.

A higher PLL bandwidth results in a faster settling behavior with lower undershoot, but is more susceptible to harmonics [5]. As can be observed from Fig. 5, the existing model (6) shows an offset resulting in a steady-state error if it is used as a linearization. Contrarily, the proposed model does not show any steady-state error and represents an accurate approximation of the nonlinear system for both parameter settings.

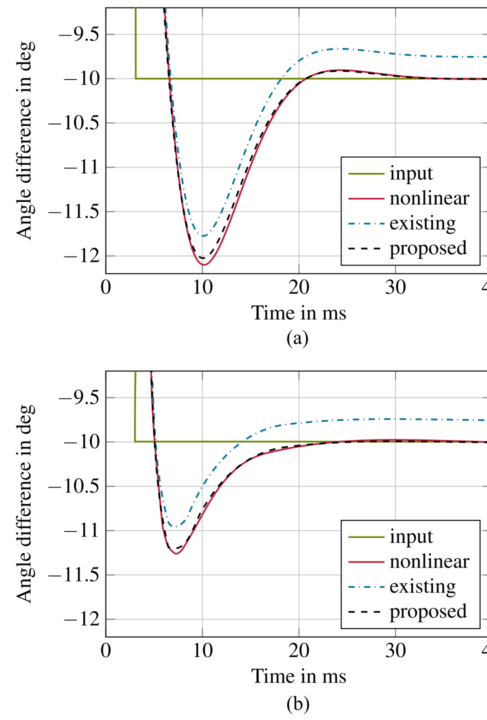

Fig. 5. Comparison of SRF-PLL models as a result of a fault, parameterized with (a) $\zeta_{\text{cl}} = 0.707, \omega_{\text{cl}} = 2\pi 50\,\frac{\text{rad}}{\text{s}}$ and (b) $\zeta_{\text{cl}} = 0.8, \omega_{\text{cl}} = 2\pi 100\,\frac{\text{rad}}{\text{s}}$.

Here, it should be noted that the model accuracy of the existing model does directly depend on the input step size. Therefore, (6) can represent a valid approximation in single converter scenarios, where small phase angle changes are preconditioned and the resulting steady-state error is permissible. However, subsequently, it should be highlighted that the application of the existing model (6) could lead to unreasonable results in studies similar to Fig. 4, where the grid reference frame is specified to be aligned with an ideal grid voltage source $\boldsymbol{v}_g$. The grid impedance $\boldsymbol{Z}_g = |\boldsymbol{Z}_g|\,e^{j\psi_g}$ introduces an additional phase angle between the grid frame and $\boldsymbol{v}_1$ inherently, and thus, the underlying assumption of (2) would no longer be satisfied, since $\hat{\theta}_1 \gg \theta_g$ (e.g., think about weak- or low-voltage grids showing extreme grid impedances). As a consequence, (6) is a worse approximation of the transient nonlinear behavior and will also show a constant offset of ψ_g.

VI. Conclusion

In this letter, the limitations of an existing SRF-PLL model were discussed. The model only approximates the nonlinear PLL behavior in special cases, where the grid reference frame is defined to be always close to the PCC voltage vector. By defining a relative phase error angle, a slightly different small-signal SRF-PLL model was proposed. A simulation study demonstrated the model applicability and accuracy. The new model overcomes the necessity to specify a scenario-dependent grid reference, and thus, is applicable to research involving single as well as multiple grid-connected DG units.

REFERENCES

[1] F. Blaabjerg, R. Teodorescu, M. Liserre, and A. V. Timbus, "Overview of control and grid synchronization for distributed power generation systems," *IEEE Trans. Ind. Electron.*, vol. 53, no. 5, pp. 1398–1409, Oct. 2006.

[2] R. Teodorescu, M. Liserre, and P. Rodriguez, *Grid Converters for Photovoltaic and Wind Power Systems*, vol. 29. Hoboken, NJ, USA: Wiley, 2011.

[3] S. I. Nanou, A. G. Papakonstantinou, and S. A. Papathanassiou, "A generic model of two-stage grid-connected PV systems with primary frequency response and inertia emulation," *Electr. Power Syst. Res.*, vol. 127, pp. 186–196, Oct. 2015.

[4] K. M. Alawasa, Y. A.-R. I. Mohamed, and W. Xu, "Modeling, analysis, and suppression of the impact of full-scale wind-power converters on subsynchronous damping," *IEEE Syst. J.*, vol. 7, no. 4, pp. 700–712, Jan. 2013.

[5] S.-K. Chung, "A phase tracking system for three phase utility interface inverters," *IEEE Trans. Power Electron.*, vol. 15, no. 3, pp. 431–438, May 2000.

[6] L. Harnefors, M. Bongiorno, and S. Lundberg, "Input-admittance calculation and shaping for controlled voltage-source converters," *IEEE Trans. Ind. Electron.*, vol. 54, no. 6, pp. 3323–3334, Nov. 2007.

[7] B. Wen, D. Boroyevich, P. Mattavelli, Z. Shen, and R. Burgos, "Influence of phase-locked loop on input admittance of three-phase voltage-source converters," in *Proc. 28th Annu. IEEE Appl. Power Electron. Conf. Expo.*, 2013, pp. 897–904.

[8] X. Wang, L. Harnefors, and F. Blaabjerg, "Unified impedance model of grid-connected voltage-source converters," *IEEE Trans. Power Electron.*, vol. 33, no. 2, pp. 1775–1787, Feb. 2018.

[9] B. Wen, D. Boroyevich, R. Burgos, P. Mattavelli, and Z. Shen, "Analysis of D-Q small-signal impedance of grid-tied inverters," *IEEE Trans. Power Electron.*, vol. 31, no. 1, pp. 675–687, Jan. 2016.

[10] C. Zhang, X. Wang, and F. Blaabjerg, "Analysis of phase-locked loop influence on the stability of single-phase grid-connected inverter," in *Proc. IEEE 6th Int. Symp. Power Electron. Distrib. Gener. Syst.*, 2015, pp. 1–8.